Chapter 2

Physics objectives

The TOTEM apparatus with its unique coverage for charged particles at high rapidities (figure 2.1, left) is the ideal tool for studying forward phenomena, including elastic and diffractive scattering. Furthermore, energy flow and particle multiplicity of inelastic events peak in the forward region (figure 2.1 right; $\eta = 3$ corresponds to a polar angle $\theta = 100\,\text{mrad}$.). About 99.5% of all non-diffractive minimum bias events and 84% of all diffractive events have charged particles within the acceptance of T1 or T2 and are thus triggerable with these detectors.

An important application is the luminosity-independent measurement of the total cross-section based on the Optical Theorem.

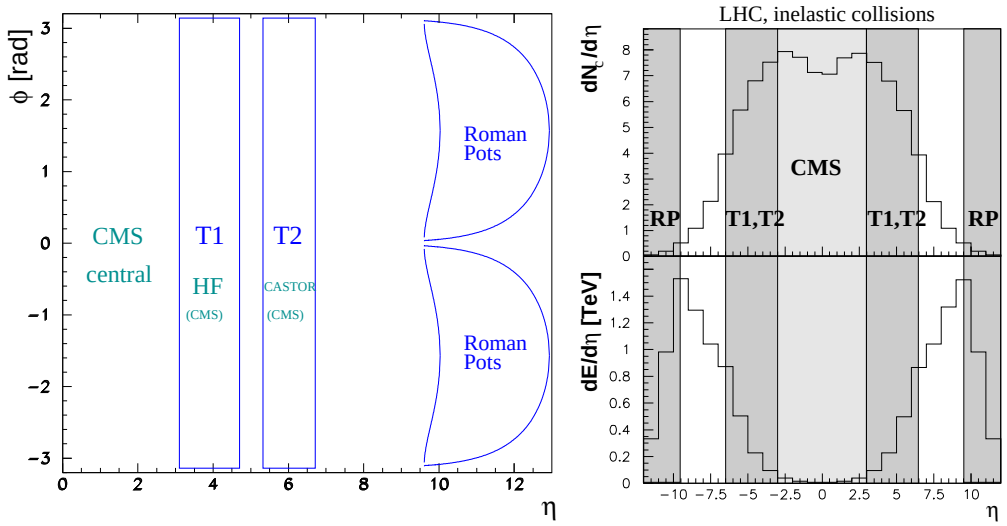

Figure 2.1: Left: coverage of different detectors in the pseudorapidity (η) - azimuthal angle (ϕ) plane. Right: charged particle multiplicity and energy flow as a function of pseudorapidity for inelastic events at $\sqrt{s} = 14\,\text{TeV}$.

2008 JINST 3 S08007

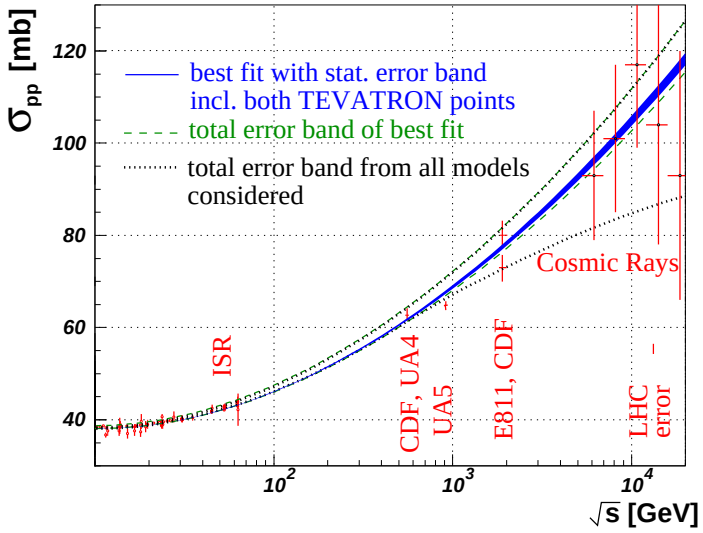

Figure 2.2: Fits from the COMPETE collaboration [5] to all available pp and $p\bar{p}$ scattering data with statistical (blue solid) and total (green dashed) error bands, the latter taking into account the discrepancy of the two Tevatron measurements. The outermost curves (dotted) give the total error band from all parameterisations considered.

2.1 Total pp cross-section

A precise measurement of the total pp cross-section σ_{tot} and of the elastic scattering over a large range in the squared four-momentum transfer t (section 2.2) is of primary importance for distinguishing between different models of soft proton interactions.

Figure 2.2 summarises the existing measurements of σ_{tot} from low energies up to collider and cosmic-ray energies. Unfortunately the large uncertainties of the cosmic-ray data and the 2.6 standard-deviations discrepancy between the two final results from the Tevatron [3, 4] make an extrapolation to higher energies uncertain, leaving a wide range for the expected value of the total cross-section at the LHC energy of $\sqrt{s} = 14\,\text{TeV}$, typically from 90 to 130 mb, depending on the model used for the extrapolation.

TOTEM will measure σ_{tot} and the luminosity $\mathscr{L}$ simultaneously by taking advantage of the Optical Theorem:

$$\mathscr{L}\,\sigma_{\text{tot}}^2 = \frac{16\pi}{1+\rho^2}\cdot\left.\frac{dN_{\text{el}}}{dt}\right|_{t=0}. \tag{2.1}$$

With the additional relation

$$\mathscr{L}\,\sigma_{\text{tot}} = N_{\text{el}} + N_{\text{inel}} \tag{2.2}$$

one obtains a system of 2 equations which can be solved for σ_{tot} or $\mathscr{L}$. The parameter

$$\rho = \frac{\mathscr{R}[f_{\text{el}}(0)]}{\mathscr{I}[f_{\text{el}}(0)]}, \tag{2.3}$$

where $f_{\rm el}(0)$ is the forward nuclear elastic amplitude, has to be taken from external theoretical predictions, e.g. [5]. Since $\rho \sim 0.14$ enters only in a $1+\rho^2$ term, its impact is small (see estimate in section 6.3.3).

Hence the quantities to be measured are the following:

- The inelastic rate $N_{\rm inel}$ consisting of non-diffractive minimum bias events ($\sim$65 mb at LHC) and diffractive events ($\sim$18 mb at LHC) which will be measured by T1 and T2.
- The total nuclear elastic rate $N_{\rm el}$ measured by the Roman Pot system.
- $dN_{\rm el}/dt|_{t=0}$: The nuclear part of the elastic cross-section extrapolated to $t = 0$ (see section 2.2). The expected uncertainty of the extrapolation depends on the acceptance for elastically scattered protons at small $|t|$-values and hence on the beam optics.

For the rate measurements it is important that all TOTEM detector systems have trigger capability.

At an early stage with non-optimal beams, TOTEM will measure the total cross-section and the luminosity with a precision of about 5%. After having understood the initial measurements and with improved beams at $\beta^* = 1540$ m (cf. chapter 3), a precision around 1% should be achievable.

Even later, a measurement of ρ via the interference between Coulomb and hadronic contributions to the elastic scattering cross-section might be attempted at a reduced centre-of-mass energy of about 8 TeV [6]. The main interest of ρ lies in its predictive power for $\sigma_{\rm tot}$ at higher energies via the dispersion relation

$$\rho(s) = \frac{\pi}{2\sigma_{\rm tot}(s)} \frac{d\sigma_{\rm tot}}{d\ln s}. \tag{2.4}$$

2.2 Elastic pp scattering

Much of the interest in large-impact-parameter collisions centres on elastic scattering and soft inelastic diffraction. High-energy elastic nucleon scattering represents one of the collision processes in which very precise data over a large energy range have been gathered. The differential cross-section of elastic pp interactions at 14 TeV, as predicted by different models [7], is given in figures 2.3 and 2.4.

The dashed graphs show the cross-section of pure nuclear scattering, i.e. neglecting the influence of the Coulomb component, which would be justified for $|t| > 10^{-3}$ GeV^2 assuming the validity of the West and Yennie description [8] of the Coulomb-nuclear interference. However, it has been shown that this formula requires $\rho(t)$ to be t independent which is not fulfilled experimentally and theoretically inconsistent [9]. Hence a second set of graphs (continuous lines) is shown taking into account the Coulomb component with a formulation of the total amplitude based on the eikonal approach. This model also describes the influence of Coulomb scattering at higher values of $|t|$, which is visible in figure 2.4 above 0.25 GeV^2.

Increasing $|t|$ means looking deeper into the proton at smaller distances. Several t-regions with different behaviour can be distinguished:

- $|t| < 6.5 \times 10^{-4}$ GeV^2 (at $\sqrt{s}$=14 TeV): The Coulomb region where elastic scattering is dominated by photon exchange: $d\sigma/dt \sim 1/t^2$.

2008 JINST 3 S08007

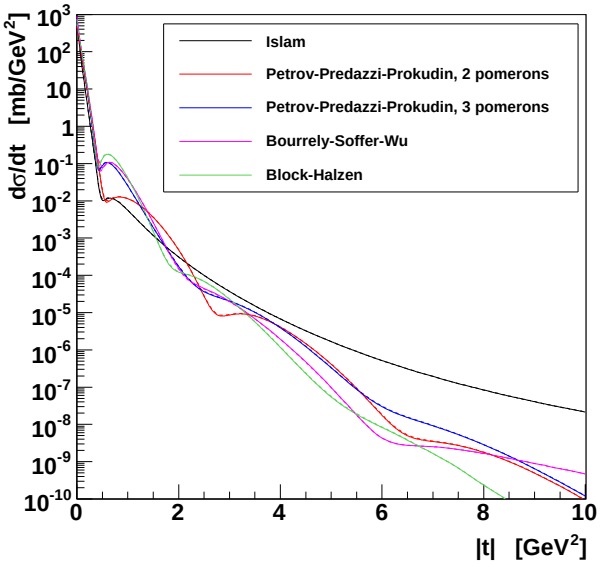

Figure 2.3: Differential cross-section of elastic scattering at $\sqrt{s} = 14\,\text{TeV}$ as predicted by various models [7]. On this scale, the cross-sections with and without the Coulomb component (continuous and dashed lines respectively) cannot be distinguished.

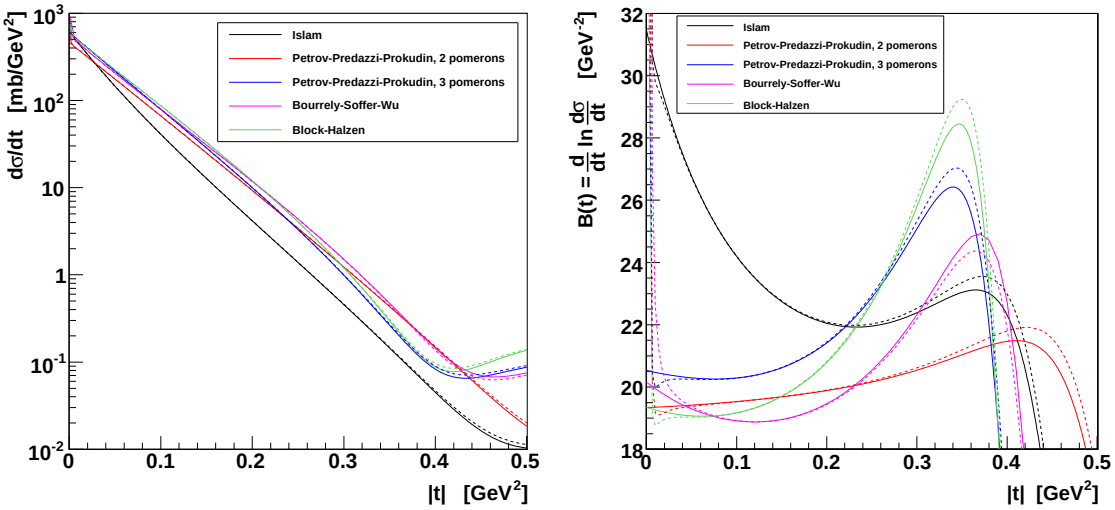

Figure 2.4: Left: differential cross-section of elastic scattering at 14 TeV as predicted by various models [7], focussing on the quasi-exponential domain at low $|t|$. Right: exponential slope of the differential cross-section. The deviations from a constant slope show how the cross-sections differ from a pure exponential shape. Continuous (dashed) lines: with (without) Coulomb interaction.

- $10^{-3}\,\mathrm{GeV}^2 < |t| < 0.5\,\mathrm{GeV}^2$: The nuclear region described in a simplified way by "single-Pomeron exchange"[1] with an approximately exponential cross-section $d\sigma/dt \sim \mathrm{e}^{-B|t|}$ (figure 2.4, left). This quasi-exponential domain is important for the extrapolation of the differential counting-rate dN_{el}/dt to $t = 0$, needed for the measurement of σ_{tot}. The t-dependence of the exponential slope $B(t) = \frac{d}{dt} \ln \frac{d\sigma}{dt}$ reveals slight model-dependent deviations from the exponential shape (figure 2.4, right). This theoretical uncertainty contributes to the systematic error of the total cross-section measurement (section 6.3.2).

- Between the above two regions, the nuclear and Coulomb scattering interfere, complicating the extrapolation of the nuclear cross-section to $t = 0$.

- $0.5\,\mathrm{GeV}^2 < |t| < 1\,\mathrm{GeV}^2$: A region exhibiting the diffractive structure of the proton.

- $|t| > 1\,\mathrm{GeV}^2$: The domain of central elastic collisions at high $|t|$, described by perturbative QCD, e.g. in terms of triple-gluon exchange with a predicted cross-section proportional to $|t|^{-8}$. The model dependence of the predictions being very pronounced in this region, measurements will be able to test the validity of the different models.

With different beam optics and running conditions (chapter 3), TOTEM will cover the $|t|$-range from $2 \times 10^{-3}\,\mathrm{GeV}^2$ to about $10\,\mathrm{GeV}^2$.

2.3 Diffraction

Diffractive scattering comprises Single Diffraction, Double Diffraction, Central Diffraction (a.k.a. "Double Pomeron Exchange"), and higher order ("Multi Pomeron") processes. Together with the elastic scattering these processes represent about 50% of the total cross-section. Many details of these processes with close ties to proton structure and low-energy QCD are still poorly understood. The majority of diffractive events (figure 2.5) exhibits intact ("leading") protons in the final state, characterised by their t and by their fractional momentum loss $\xi \equiv \Delta p/p$. Depending on the beam optics (chapter 3) most of these protons can be detected in Roman Pot detectors far away from the interaction point. Already at an early stage, TOTEM will be able to measure ξ-, t- and mass-distributions in soft Double Pomeron and Single Diffractive events. The full structure of diffractive events with one or more sizeable rapidity gaps in the particle distributions (figure 2.5) will be optimally accessible when the detectors of CMS and TOTEM will be combined for common data taking with an unprecedented rapidity coverage, as discussed in [2].

[1] Nuclear elastic and diffractive scattering are characterised by the exchange of hadronic colour singlets, for which the Pomeron is one model.

2008 JINST 3 S08007

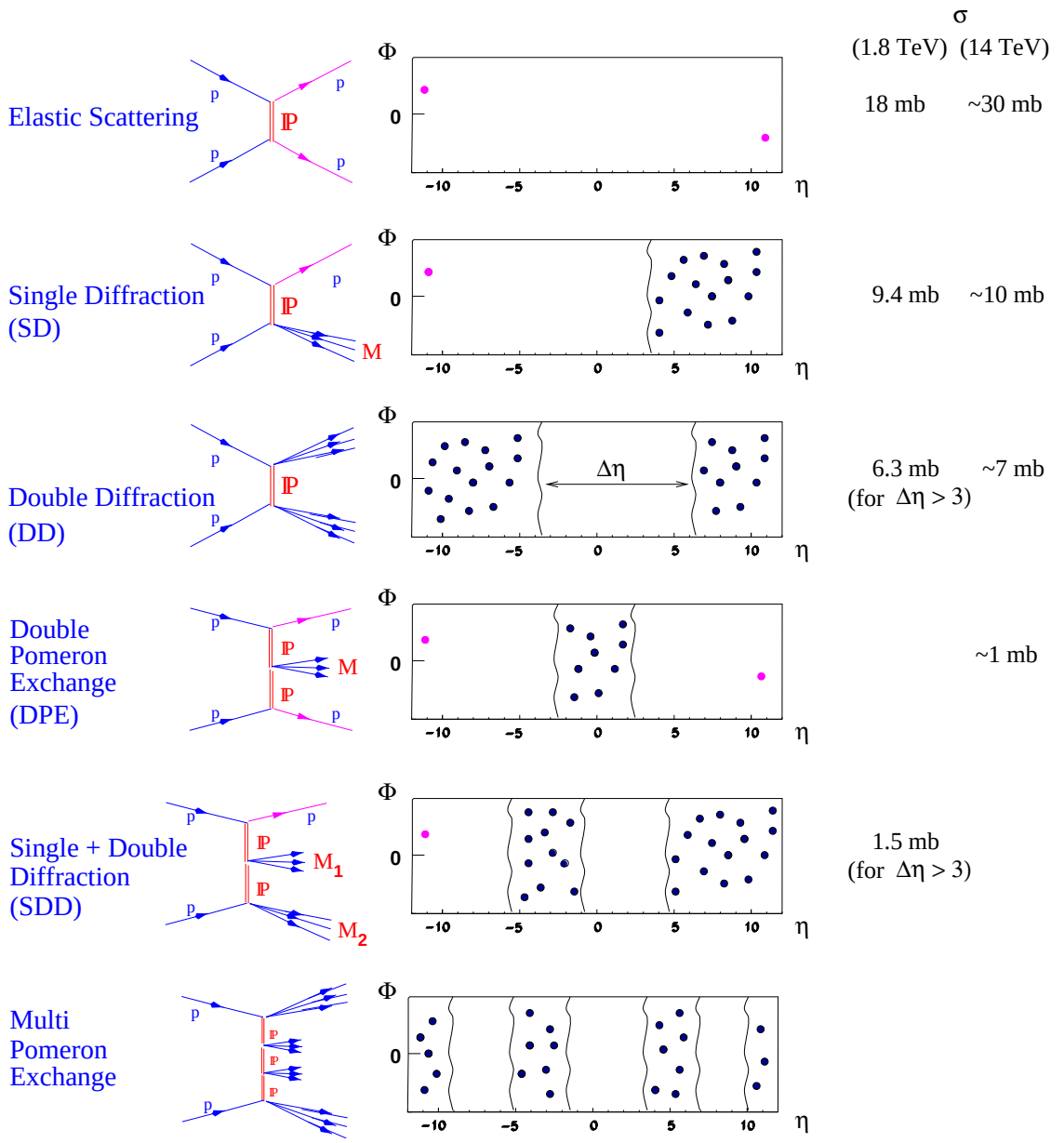

Figure 2.5: Diffractive process classes and their cross-sections measured at Tevatron and estimated for the LHC.